Surface Science 644 (2016) 91–94

Contents lists available at ScienceDirect

Surface Science

journal homepage: www.elsevier.com/locate/susc

# Electronic end-states in platinum atom chains

René Heimbuch *,[1], Hasan Ateşçi [1], Iris Slootheer, Harold J.W. Zandvliet

*Physics of Interfaces and Nanomaterials, MESA + Institute for Nanotechnology, P. O. Box 217, 7500 AE Enschede, The Netherlands*

ARTICLE INFO

*Article history:*
Received 22 July 2015
Accepted 21 September 2015
Available online 30 September 2015

*Keywords:*
Nanowires
End states
Scanning tunneling spectroscopy
Tight-binding

ABSTRACT

We investigated electronic surface states in platinum atom chains grown on Ge(001). Scanning tunneling microscopy/spectroscopy was used to record the electronic landscape on atomic platinum chains. High-resolution spatial maps of individual Pt-dimers near the termini of the chains revealed a difference in the electronic structure between the end dimer region and the chains bulk region. Experiments and tight-binding calculations show a one-dimensional character of the electronic states, decaying rapidly into the chains.

© 2015 Elsevier B.V. All rights reserved.

## 1. Introduction

Nanowires, nanoscopic structures with a very high aspect ratio, can be assembled on substrates using various material compositions. On the forefront of these, silicon (Si) and germanium (Ge) are the most widely used substrates. A broad range of possible materials is known to induce the growth of nanowires on Si and Ge. Under high investigation are nanowires, induced from rare earths [1], transition metals and post-transition metals [2]. Especially 5d transition metals, such as gold (Au) [3–6], platinum (Pt) [7] and iridium (Ir) received much attention over the last decade. Pt atom chain assemblies are ideal systems to study, for instance, quantum confinement [8–10] and Peierls instabilities [11,12].

The structural and electronic properties make the nanowire arrays ideal anchors for molecules, that are of interest to molecular electronics. By capturing a single molecule between a nanowire and the apex of a scanning tunneling microscope tip the transport properties of an individual molecule can be determined [13–18].

Low dimensional electronic states have been of great interest in nanoscience and nanotechnology [19–22]. Quantum dots [23–26] and atomic nanowires are on the forefront of science of low-dimensional physics. While quantum dots are mainly used to store and release low quantities of electric charge, nanowires are heavily investigated because of their importance for electronic transport [27,28]. However, one-dimensional atomic wires can also host zero-dimensional electronic states. Crain and Pierce studied Au nanostructures on Si (553) and showed the existence of zero-dimensional end-states at the edges of these structures [29].

In this work we demonstrate an end-state effect of the electronic states in proximity to the termini inside Pt atom chains. These self-assembling chains were grown on a Ge(001) surface [30,7,8,31,32]. These effects are investigated with scanning tunneling microscopy and spectroscopy (STM and STS), supported by tight binding calculations to study the origin of the state and its dimensionality.

## 2. Experimental details

The experiments were performed in a dedicated ultra-high vacuum system equipped with an Omicron low-temperature STM. The Ge(001) samples are cut from nominally flat, 3 in. by 0.3 mm, single-side polished, nearly intrinsic n-type wafers. After cutting, the samples were thoroughly cleaned with isopropanol alcohol, before inserting them into the ultra-high vacuum system. First the Ge(001) samples were outgassed for at least 12 h at a temperature of 750–800 K. Subsequently, we cleaned the Ge(001) samples by applying cycles of argon ion bombardment (500 eV, 20 min), followed by annealing at temperatures of 1100 (±25) K. After several of these cleaning cycles, the Ge(001) samples were atomically clean and exhibited a well-ordered dimer reconstructed surface [33,30]. Subsequently, an equivalent of 0.2–0.5 monolayers of Pt was deposited onto the substrate at room temperature. Pt was evaporated by resistively heating high purity Pt (99.995%) wires, wrapped around a tungsten wire. Immediately after deposition the sample was flash-annealed to 1050 (±25) K three times and then cooled down to room temperature before placing it into the STM for imaging. All experiments are performed at 77 K.

## 3. Results and discussion

Fig. 1 shows a scanning tunneling microscope image of an array of self-organizing atomic Pt chains on Ge(001). The most abundant

* Corresponding author.
*E-mail address:* r.heimbuch@utwente.nl (R. Heimbuch).
[1] These authors contributed equally to this work.

http://dx.doi.org/10.1016/j.susc.2015.09.019
0039-6028/© 2015 Elsevier B.V. All rights reserved.

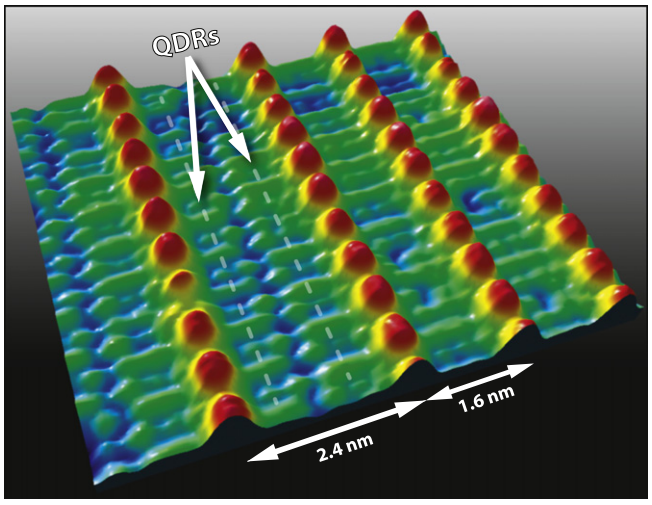


**Fig. 1.** STM image of Pt atom chains on a Ge(001) surface with separations of 1.6 nm and 2.4 nm. Quasi dimer rows are visible in the troughs. The image was recorded at 77 K at a setpoint current of 0.5 nA and a bias voltage of 1.5 V.

nearest-neighbor spacing between the atomic Pt chains is 1.6 nm, however larger spacings (e.g. 2.4 nm) can occur [34,7]. In this low temperature STM image, the spacing of 2.4 nm reveals that in every second Ge–Ge dimer one Ge atom is replaced by a Pt atom, forming the so called quasi dimer rows (QDRs) [7]. The adjacent QDR shows the same alteration, however the registry is shifted by one dimer, giving the configuration a zipper-like appearance.

At room temperature, the atomic chains are comprised of symmetric dimers yielding a 2× periodicity. Scanning tunneling spectroscopy measurements reveal that the atomic chains are metallic at room temperature. Upon cooling down to cryogenic temperatures the atomic chains, when present in an arrangement of multiple chains (see Fig. 1 for an example of such a patch of chains), undergo a doubling of the periodicity and the density of states at the Fermi level is suppressed [11]. This transition is interpreted as a Peierls transition. The Peierls phase transition temperature is intimately related to the coupling to the environment. The weaker the coupling, the lower the Peierls phase transition temperature. The Peierls transition temperature for an ideal 1D system is 0 K [12]. For chains not present in patches, i.e. isolated chains with no neighboring chains, the transition temperature can be lower than 4.7 K, since isolated Pt atom chains still exhibit a 2× periodicity at 4.7 K.

We investigated the electronic landscape of the Pt chains at 77 K. For this experiment, we focus on a small group of nanowires within a larger patch. The selected area can be seen in Fig. 2. Pt atoms, missing within the chain, restrict the wires in length. At the selected location, multiple short wires in close proximity to each other can be found, that all have a missing atom or dimer along the chains. This makes it possible to study the electronic states at the end of and along many smaller nanowires within one experiment, ensuring uniform experimental conditions.

An STM image of several Pt chains is shown in Fig. 1. The typical distance between the individual nanowires is 1.6 nm. This distance can be larger, however it will always be a multiple of 0.8 nm at a 1.6 nm minimum, due to the surface reconstruction on the underlying substrate. The nanowires can accumulate to large, well-defined patches or appear in small groups. This is influenced by the density of defects on the surface and the coverage of Pt.

Scanning tunneling spectroscopy was performed on this specific region, with high spatial resolution, in order to achieve satisfactory statistics. For this the tip was parked at every point on a 75 by 75 point grid raster. The feedback loop was then switched off at each grid point and the voltage was swept between 1 V and −1 V. The setpoint for the measurements was always 1 V at 180 pA tunneling current. Six wires have been selected for a detailed investigation of their electronic

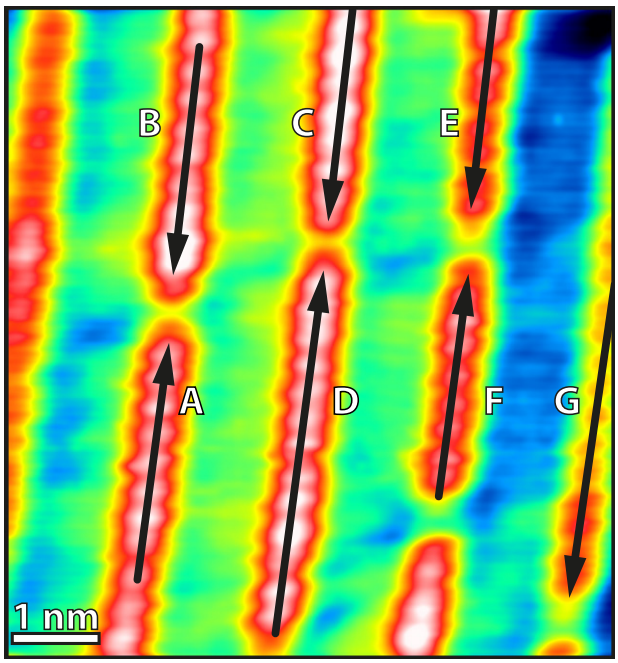


**Fig. 2.** A 7 nm × 7 nm STM image of a set of Pt atom chains labeled A to G, recorded at 77 K. STS was performed on each of these wires in order to examine the spatial dependence of electronic states in proximity to the end of the wires (end dimer is indicated by the arrow head). The bias voltage was 1 V for a current setpoint of 180 pA.

characteristics, in the center of the image. For this, we divided each wire into its respective dimers and average all the spectroscopy data for each dimer. For the three top wires (B, C and E in Fig. 2) the "End Dimer" was defined as the last dimer at the bottom of the wire. All subsequent dimers in the chain are labeled by position relative to the end dimer (e.g. "1st Bulk Dimer" to "4th Bulk Dimer 4") upwards from the end dimer for the wire B, C and E. Similarly the end dimers of the three bottom wires (A, D and F in Fig. 2) were defined as the top most dimers in the chains with the bulk dimers counting up in the downwards direction. All of the $I(V)$ curves were averaged for each respective dimer.

Several peaks in the local density of states (LDOS) can be identified on the positive bias side of the spectra. The LDOS was determined by normalizing the differential conductivity dI(V)/dV with I(V)/V. Two peaks are most pronounced: one peak is located in a bias window between −200 mV and −310 mV (Peak 1 in Fig. 3). The other (Peak 2 in Fig. 3) is located between −720 mV and −650 mV. The most remarkable aspects of these crests are, that the maximum of Peak 1

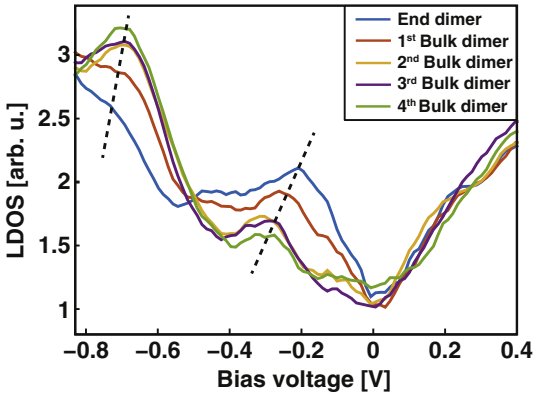


**Fig. 3.** LDOS measurements performed on Pt atom chains. Each curve represents the LDOS of a specific dimer in the chain from the end dimer counting up to four bulk dimers. The measurements were taken at a setpoint current of 180 pA and voltage of 1 V.

becomes smaller the further we move onto dimers away from the edge of the chain. We define this electronic state as the chain's "end state". Furthermore the peak position shifts towards lower energies. Contrary to this, Peak 2 decreases in absolute height with increasing dimer position and shifts towards higher energies. The position and scale the electronic states reach with higher dimer number stalls for the remainder of the chain (4th dimer onwards) until the other terminus is approached. At the location of the defect, i.e. the gap between two end dimers, the electronic states are not present.

In order to improve our understanding of the experimental results we reconstructed the spectroscopic data using numerical methods. For this we chose to model the LDOS, using simple nearest neighbor tight-binding calculations [35,12]. This has the advantage to provide insights regarding the electronic states, with relatively basic calculations that do not require complex algorithms and large computing power. The LDOS of a short chain of atoms can thus be reconstructed easily. The basis of the used model is a chain of few atoms with no interaction with the substrate (see Fig. 4).

The tight-binding Hamiltonian in tri-diagonal form, for a one-dimensional crystal, consisting of equal atoms is given by

$$\mathcal{H} = \sum_n a_n |f_n\rangle\langle f_n| + \sum_n b_{n+1}\left[|f_n\rangle\langle f_{n+1}| + |f_{n+1}\rangle\langle f_n|\right] \tag{1}$$

with diagonal matrix elements $a_n$ and off-diagonal $b_n$ for the binding energy and the hopping integrals, respectively [35]. The Hamiltonian is based on localized orbitals of the form of

$$|f_n\rangle = |\phi_a(x-x_n)\rangle\,. \tag{2}$$

$\phi_a$ is the atomic orbital function of the atoms at the atom site $x_n$. A straightforward approach to the calculation can be achieved by describing the Hamiltonian in a matrix. This has the advantage of an easily accessible Green's function for the tri-diagonal operators [35].

The Hamiltonian, for example for a five atom long chain, can be described by the following matrix.

$$M = \begin{bmatrix} E_0 & t_{end} & 0 & 0 & 0 \\ t_{end} & E_0 & t & 0 & 0 \\ 0 & t & E_0 & t & 0 \\ 0 & 0 & t & E_0 & t_{end} \\ 0 & 0 & 0 & t_{end} & E_0 \end{bmatrix}. \tag{3}$$

Where $E_0$ is the binding energy of the electron, $t$ is the nearest neighbor hopping integral of the bulk electrons and $t_{end}$ is the hopping integral of the electrons at the end of the chain (see Fig. 4). The electron energy $E$ along the bulk of wire can be calculated using

$$E = E_0 + 2t\cdot\cos(ka)\,. \tag{4}$$

Where $k$ is the wave vector and $a$ is the lattice constant. Taking into account the change in the periodic potential at each end of the wires, the electron energy at these locations changes to

$$E = E_0 + 2t_{end}\cdot\cos(ka)\,. \tag{5}$$

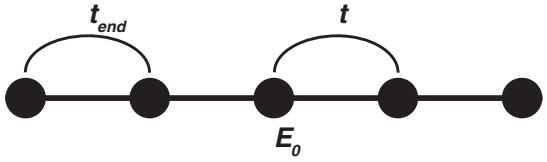


**Fig. 4.** Illustration of a one-dimensional atomic chain used for tight-binding calculations. Electrons in such a system have the binding energy $E_0$ and the hopping integrals $t_{end}$ and $t$ describe the interaction to the electrons' nearest neighbor.

For a matrix with the energies as diagonal matrix elements, the DOS $n_0$ projected on a state $|f_0$ is defined as

$$n_0(E) = \sum_m |\langle f_0|\Psi_m\rangle|^2\delta(E-E_m)\,. \tag{6}$$

Usefully, the (retarded) Green's function for the Hamiltonian can be defined as

$$G(E+i\epsilon) = \frac{1}{E+i\epsilon-\mathcal{H}} \tag{7}$$

with $i\epsilon$ being an infinitesimal small positive imaginary part added to the energy. In many-body-theory, the Green's function allows the connection of the Hamiltonian with the DOS the atomic system [35]:

$$\begin{aligned} G_{00}(E+i\epsilon) &= \left\langle f_0\left|\frac{1}{E+i\epsilon-\mathcal{H}}\right|f_0\right\rangle \\ &= \sum_m |\langle f_0|\Psi_m\rangle|^2\,\frac{E-E_m-i\epsilon}{(E-E_m)^2+\epsilon^2}\,. \end{aligned} \tag{8}$$

The DOS of each atomic position in the wire can then be calculated by its appropriate spectral function:

$$n_0(E) = -\frac{1}{\pi}\lim_{\epsilon\to 0^+}\Im G_{00}(E+i\epsilon)\,. \tag{9}$$

Fig. 5 shows the results of such a calculation that has manually been fitted to achieve the best agreement to our experimental results. Here we calculated the LDOS using a chain of ten atoms with a lattice constant of 0.4 nm. The binding energy $E_0$ is 503.1 meV. The hopping integrals where determined to be $t = 530.5$ meV for the sites in the bulk of the wire and $t_{end} = 124.8$ meV for the interaction between the end atom and its nearest neighbor.

These calculations are a rather crude estimate of the LDOS of the system, spin and electron interaction was neglected as well as a slight deformation of the single particle eigenstates and energy levels near at the edges. However, one must keep in mind that the approach was intentionally left simple to increase the fitting and calculation capability and focus on reproducing the physical trends, of which tight-binding calculations are well suited for. One can see a clear agreement in Fig. 5 in the following points; firstly, the LDOS exhibits a number of peaks, both at the negative and at the positive side of the Fermi level. It is important to point out, that the setpoint is located at positive bias and the feedback mechanism of the STM regulates the current before the $I(V)$ curves are recorded. Because of this, features on the side of the sign of the bias voltage are less pronounced than on the opposite site. However, a distinct peak in the LDOS can still be observed at around 220 mV in Fig. 3. The absolute peak position varies, as is the case in the simulation.

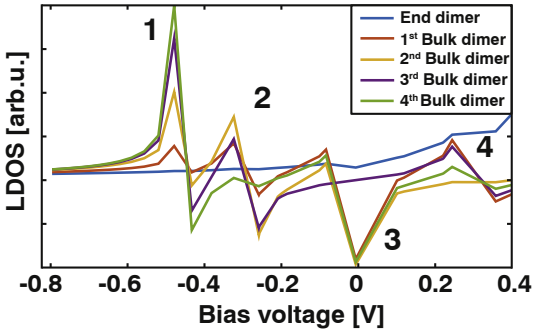


**Fig. 5.** Tight-binding calculations of a short chain of atoms. Distinct features of the LDOS can be reproduced, such as various peaks (1, 2 and 4) and the minimum LDOS at zero-bias (3).

Unfortunately, we cannot draw a definite conclusion for the dimer dependence of this peak height, at that energy, because the experiment shows only a small variation, whereas the simulation depicts a clearer picture, due to it not being affected by the setpoint characteristics of the measurement.

The same characteristics could be reproduced in the tight-binding model. Two peaks can be observed on the negative side as well as the minimum at zero bias (Fig. 3). Even though only a small number of parameters have to be fitted within the calculations, we were able to match the model in such a way that the peak heights follow the same trend as to what the experiments show. The peak associated with the end state shrinks with higher dimer number in the bulk of the chain. The peak furthest from zero bias behaves in the opposite way. The simplicity of the calculations however, did not allow for a reproduction of the shift in energy of the peaks. The absolute positions of the peaks are very sensitive to small changes in the fitting parameters. Regarding the approximating nature of the fit, we therefore focus on the model's ability to reproduce the defining trends of the electronic structure, rather than a forced match at the cost of physical meaning. The fact that one crest shrinks while the other one grows can be allocated to a asymmetric charge distribution, caused by the morphological asymmetry in the Pt atomic chains. This asymmetry is caused by the missing nearest-neighbor of the last dimer in the Pt chains. As we indisputably see, the end state does penetrate into the bulk where it quickly diminishes. A zero-dimensional electronic state can therefore be ruled out because of this behavior. We can safely assume this end-state in atomic Pt chains to be a one-dimensional electronic state, decaying rapidly into the chain.

## 4. Summary

We have shown that an array of self-assembled Pt atom chains can be used to investigate end state effects at the edge of each chain. We used an assembly of short chains to map the electronic density of states as a function of position on the wires. The measured results show clear electronic states that change in amplitude and position the closer the dimer is located to the end of the chain. These electronic states were reproduced in a tight-binding model based simulation. The fact that the trend of these states can be reproduced using tight-binding methods, with introducing a separate hopping integral for the ends of the chain, undoubtedly supports the theory of the end-states being caused by an asymmetry in the charge distribution.

## Acknowledgment

We would like to thank the Stichting voor Fundamenteel Onderzoek der Materie (FOM, 10ODE01) for financial support.

## References

[1] V. Iancu, P.R.C. Kent, S. Hus, H. Hu, C.G. Zeng, H.H. Weitering, J. Phys. Condens. Matter 25 (2013) 014011.
[2] M. Naitoh, H. Shimaya, S. Nishigaki, N. Oishi, F. Shoji, Surf. Sci. 377-379 (1997) 899 (European Conference on Surface Science).
[3] J. Wang, M. Li, E.I. Altman, Phys. Rev. B: Condens. Matter Mater. Phys. 70 (2004) 233312.
[4] R. Heimbuch, M. Kuzmin, H.J.W. Zandvliet, Nat. Phys. 8 (2012) 697.
[5] C. Blumenstein, J. Schäfer, S. Mietke, S. Meyer, A. Dollinger, M. Lochner, X.Y. Cui, L. Patthey, R. Matzdorf, R. Claessen, Nat. Phys. 7 (2011) 776.
[6] J. Park, K. Nakatsuji, T.-H. Kim, S.K. Song, F. Komori, H.W. Yeom, Phys. Rev. B 90 (2014) 165410.
[7] O. Gurlu, O. Adam, H.J.W. Zandvliet, B. Poelsema, Appl. Phys. Lett. 83 (2003) 4610.
[8] N. Oncel, A. van Houselt, J. Huijben, A.-S. Hallbäck, O. Gurlu, H.J.W. Zandvliet, B. Poelsema, Phys. Rev. Lett. 95 (2005) 116801.
[9] A. van Houselt, N. Oncel, B. Poelsema, H.J.W. Zandvliet, Nano Lett. 6 (2006) 1439.
[10] R. Heimbuch, A. van Houselt, M. Farmanbar, G. Brocks, H. Zandvliet, J. Phys. Condens. Matter 25 (2013) 014014.
[11] A. van Houselt, T. Gnielka, J.M.J. Aan de Brugh, N. Oncel, D. Kockmann, R. Heid, K. Bohnen, B. Poelsema, H.J.W. Zandvliet, Surf. Sci. 602 (2008) 1731.
[12] C. Kittel, in: S. Johnson (Ed.), Introduction to Solid State Physics, 8th edWiley India Pvt. Limited, 2007.
[13] S.J. van der Molen, P. Liljeroth, J. Phys. Condens. Matter 22 (2010) 133001.
[14] A. Kumar, R. Heimbuch, B. Poelsema, H.J.W. Zandvliet, J. Phys. Condens. Matter 24 (2012) 082201.
[15] A. Saedi, R.P. Berkelaar, A. Kumar, B. Poelsema, H.J.W. Zandvliet, Phys. Rev. B 82 (2010) 165306.
[16] R.P. Berkelaar, H. Söde, T.F. Mocking, A. Kumar, B. Poelsema, H.J.W. Zandvliet, J. Phys. Chem. C 115 (2011) 2268.
[17] K. Sotthewes, R. Heimbuch, H.J.W. Zandvliet, J. Chem. Phys. 139 (2013) 214709.
[18] K. Sotthewes, V. Geskin, R. Heimbuch, A. Kumar, H.J.W. Zandvliet, APL Mater. 2 (2014) 010701.
[19] N.D. Mermin, H. Wagner, Phys. Rev. Lett. 17 (1966) 1133.
[20] P. Gambardella, A. Dallmeyer, K. Maiti, M.C. Malagoli, W. Eberhardt, K. Kern, C. Carbone, Nature 416 (2002) 301.
[21] A.I. Yanson, G. Rubio Bollinger, H.E. van den Brom, N. Agraït, J.M. van Ruitenbeek, Nature 395 (1998) 783.
[22] N. Nilius, T.H. Wallis, W. Ho, Science 297 (2002) 1853.
[23] D. Vasudevan, R. Gaddam, A. Trinchi, I. Cole, J. Alloys Compd. 636 (2015) 395.
[24] B. Sothmann, R. Sánchez, A.d. Jordan, Nanotechnology 26 (2015) 23.
[25] K. Dohnalová, T. Gregorkiewicz, K. Kusová, J. Phys. Condens. Matter 26 (2014) 28.
[26] J. Albero, J. Clifford, E.b. Palomares, Coord. Chem. Rev. 263-264 (2014) 53.
[27] C.L. Kane, M.P.A. Fisher, Phys. Rev. Lett. 68 (1992) 1220.
[28] J. Schäfer, S. Meyer, C. Blumenstein, K. Roensch, R. Claessen, S. Mietke, M. Klinke, T. Podlich, R. Matzdorf, A.A. Stekolnikov, S. Sauer, F. Bechstedt, New J. Phys. 11 (2009) 125011.
[29] J.N. Crain, D.T. Pierce, Science 307 (2005) 703.
[30] H.J.W. Zandvliet, Phys. Rep. 388 (2003) 1.
[31] D.E.P. Vanpoucke, G. Brocks, Phys. Rev. B 77 (2008) 241308.
[32] D.E.P. Vanpoucke, G. Brocks, Phys. Rev. B 81 (2010) 085410.
[33] H.J.W. Zandvliet, B.S. Swartzentruber, W. Wulfhekel, B.J. Hattink, B. Poelsema, Phys. Rev. B 57 (1998) R6803.
[34] N. Oncel, W.J. van Beek, J. Huijben, B. Poelsema, H.J. Zandvliet, Surf. Sci. 600 (2006) 4690.
[35] G. Grosso, G. Parravicini, Solid State Physics, Elsevier Science, 2000.